Original Article

A Collagen-Targeted Biomimetic RGD Peptide to Promote Osteogenesis

Rick Visser, PhD,[1–3] Pilar M. Arrabal, PhD,[1–3] Leonor Santos-Ruiz, PhD,[1–3]
Raul Fernandez-Barranco, BSc,[1,3] Jose Becerra, PhD,[1–3] and Manuel Cifuentes, PhD[1–3]

Osteogenesis is a complex, multifactorial process in which many different signals interact. The bone morphogenetic proteins (BMPs) are the most potent inducers of osteoblastic differentiation, although very high doses of BMPs in combination with collagen type I formulations have to be used for clinical applications. Although integrin-binding arginine-glycine-aspartic acid (RGD) biomimetic peptides have shown some promising abilities to promote the attachment of cells to biomaterials and to direct their differentiation, the linking of these peptides to collagen sponges usually implies chemical manipulation steps. In this study, we describe the design and characterization of a synthetic collagen-targeted RGD biomimetic (CBD-RGD) peptide formed from a collagen-binding domain derived from the von Willebrand factor and the integrin-binding RGD sequence. This peptide was demonstrated to bind to absorbable collagen type I sponges (ACSs) without performing any chemical linking, and to induce the differentiation of MC3T3-E1 mouse preosteoblasts and rat bone marrow-derived mesenchymal stem cells. Furthermore, *in vivo* experiments showed that ACSs functionalized with CBD-RGD and loaded with a subfunctional dose of BMP-2-formed ectopic bone in rats, while nonfunctionalized sponges loaded with the same amount of BMP-2 did not. These results indicate that the combination of this biomimetic peptide with the currently used collagen + BMP system might be a promising approach to improve osteogenesis and to reduce the doses of BMPs needed in clinical orthopedics.

Introduction

MOST MEMBERS OF the bone morphogenetic protein (BMP) subfamily are potent osteogenic growth factors, some of them being approved by the Food and Drug Administration (FDA) and the European Medicines Agency (EMA) to be used, in combination with collagen type I formulations, in clinical orthopedics. In particular, BMP-2 and -7 combined with absorbable collagen type I have demonstrated to be effective for the treatment of severe tibial fractures and posterolateral spinal fusions.[1–5] Although the use of BMPs is considered safe at short term, the very high doses that need to be applied make these treatments not only very expensive for healthcare providers,[6] but also raises questions about their safety at longer terms. In fact, a single administration of allogeneic BMPs can promote the recruitment of macrophages, lymphocytes, and plasma cells, as well as activate a moderate production of anti-BMP antibodies.[7] Trying to overcome these inconveniences, different researchers have focused on developing new strategies to improve the currently used collagen + BMP systems by modifying the carrier,[8,9] producing recombinant BMPs with new features,[10] complementing the system with additional cytokines[11–13] or developing multiphasic biomaterials to mimic the temporal profile in which different growth factors act during natural bone healing.[13,14]

Although the BMPs are the only growth factors known to have the ability to induce ectopic bone formation,[15,16] osteogenesis is a complex, multifactorial process, with a great variety of signals modulating the osteogenic cell behavior. One important stimulus for osteoblast proliferation and differentiation, as well as for matrix mineralization, is the adhesion of the cells to the extracellular matrix (ECM), this process being primarily mediated by integrins. When these transmembrane receptors recognize specific motifs present in many ECM proteins, they cluster together to form focal adhesions, which are associated with the actin cytoskeleton. The formation of focal adhesions does not only affect cell adhesion and migration, but can also be responsible for triggering intracellular signaling pathways that mediate mesenchymal cell commitment and osteoblast differentiation.[17] Among the great variety of integrin-recognition motifs identified to date, the arginine-glycine-aspartic acid (RGD) sequence, present in certain ECM molecules, is one of the most studied, with several groups having reported

[1]Department of Cell Biology, Genetics and Physiology, Faculty of Science, University of Malaga, Malaga, Spain.
[2]Networking Research Center on Bioengineering, Biomaterials and Nanomedicine, (CIBER-BBN), Malaga, Spain.
[3]Andalusian Center for Nanomedicine and Biotechnology (BIONAND), Parque Tecnologico de Andalucia, Malaga, Spain.

enhanced cell adhesion and/or osseointegration of titanium implants functionalized with RGD-biomimetic peptides.[18–20] Furthermore, the combination of RGD-biomimetic peptides with BMP-2 or BMP-2-derived peptides have been shown to enhance the proliferation and the expression of osteogenic markers by human mesenchymal stem cells[21] and to stimulate their differentiation *in vivo*.[22]

To exert its effect, RGD-biomimetic peptides have to be anchored to the biomaterial of election, having a broad range of approaches been used to achieve this for many different implantable materials. For the functionalization of titanium implants with RGD-peptides, strategies such as simple adsorption[23] or chemical linking through gold–thiol chemistry[24] or electrodeposited PEG[25] have been carried out. In the case of collagen type I, functionalization with this type of biomimetic peptides have been done through chemical procedures such as using thiol or phosphonate anchors,[26] periodate activation[27] or hetero-bifunctional coupling agents.[28] To avoid any chemical modification to functionalize absorbable collagen type I sponges (ACSs) with RGD-biomimetic peptides, we have designed a synthetic peptide formed from a decapeptidic collagen-binding domain (CBD) modified from the von Willebrand factor (vWF) with an RGD domain at the C-terminus. This CBD has been previously used to produce recombinant fusion proteins with growth factors involved in the osteogenic process, such as transforming growth factor-beta,[29,30] basic fibroblast growth factor,[31] or BMP-2,[10] with all these proteins maintaining their biological activities and displaying an enhanced affinity to collagen type I. The here described collagen-targeted RGD biomimetic (CBD-RGD) peptide would allow simple, one-step functionalization of ACSs without any further manipulation of the sponges. In this study, we have tested the affinity of the CBD-RGD peptide to ACSs and its activity on cultured MC3T3-E1 mouse preosteoblasts and rat bone marrow-derived mesenchymal stem cells (MSCs). Furthermore, we have studied the effect of CBD-RGD-functionalized ACSs on ectopic bone formation in rats when used in combination with a subfunctional dose of BMP-2.

Materials and Methods

Cells, recombinant proteins, and antibodies

MC3T3-E1 mouse preosteoblasts (#99072810) were obtained from the European Collection of Cell Cultures (ECACC). Rat MSCs were isolated from one 8-week-old male Fisher-344 rat. Briefly, the animal was anesthetized with a medetomidine/ketamine cocktail, sacrificed by decapitation, and its femora excised. The epiphyses were removed and the bone marrow was flushed out of the diaphyses with alpha-MEM (Sigma-Aldrich, Steinheim, Germany). Erythrocytes were removed by incubating the sample for 10 min in a red blood cell lysing buffer (Sigma-Aldrich). Afterward, the remaining cells were expanded as monolayers in T-75 culture flasks (Nunclon; Nunc, Roskilde, Denmark) in alpha-MEM supplemented with 10% fetal bovine serum (FBS), 100 U/mL penicillin, and 100 μg/mL streptomycin, with a change of medium at day 3 to remove the nonadherent cells. The cells used for the *in vitro* assays were at passage 3–4. Recombinant human BMP-2 produced in CHO cells was purchased from R&D Systems (Minneapolis, MN) and handled according to the manufacturer's instructions. The biomimetic CBD-RGD

peptide (WREPSFMALSGRGDS) was synthesized by peptide 2.0 (Chantilly, VA) and supplied purified to >98.5% by high-performance liquid chromatography. Reconstitution of the peptide was done with a 25 mM phosphate buffer (PB), pH 6.2 to a concentration of 1 mg/mL. The anti-osteopontin monoclonal antibody was obtained from the Developmental Studies Hybridoma Bank (Iowa City, IA) and the anti-mouse IgG biotinylated monoclonal antibody was from Abcam (Cambridge, MA). Monoclonal anti-vinculin IgG and phalloidin-TRITC were from Sigma-Aldrich and the goat anti-mouse IgG conjugated to Alexa 488 from Invitrogen.

Saturation of ACSs with CBD-RGD

To determine the amount of CBD-RGD that can be retained by a certain amount of collagen type I, an absorbable collagen sponge sheet (from highly pure, bovine skin, native collagen, kindly provided by Dr. M.E. Nimni; US patent 5374539) was cut into discs (5 mm diameter, 1 mm thickness). These absorbable collagen sponges were extensively washed with phosphate-buffered saline (PBS) and let to dry for several hours in a laminar flow cabinet. Once dried, the ACSs were loaded with 1 or 5 μg CBD-RGD in 10 μL of PBS and allowed to dry again. To quantify the unbound molecules of CBD-RGD, the ACSs were sequentially washed six times with 15 μL of PBS, and the concentration of CBD-RGD in the washing fractions was estimated by spectrophotometry at 205 nm. Control ACSs, loaded with vehicle only, were treated in the same way and used for blanking. For easier graphic interpretation, the amount of washed out peptide in a certain fraction was summed to the amounts measured in all preceding wash fractions, thus always representing the totality of washed out peptide ($n = 4$).

To allow visualization of the molecules that are washed out of the sponges or retained by these, the above-described experiment was repeated using biotinylated CBD-RGD. For this purpose, biotin was linked to the N-terminus of the peptide using a commercial kit (EZ-Link Sulfo-NHS-Biotinylation Kit; Pierce, Rockford, IL). The biotinylated peptides were purified by passing them through a polyacrylamide desalting column (Pierce) and the molar-to-molar biotin:CBD-RGD ratio was determined using a HABA-based kit (Biotin Quantitation Kit; Pierce). After loading and washing the ACSs as described earlier, the complete wash volumes were loaded on a PVDF sheet for detection of the peptides using streptavidin-peroxidase polymer (Sigma-Aldrich) and ECL Western Blotting Detection Reagents (GE Healthcare, Uppsala, Sweden). Similarly, the washed ACSs were also incubated with the streptavidin-peroxidase polymer for visualization of the peptides that remained bound to them. ACSs loaded with nonbiotinylated CBD-RGD were used as controls ($n = 3$).

Finally, to test the stability of the peptide binding to the sponges, ACSs were loaded with 1 μg of biotinylated CBD-RGD and extensively washed with PBS for 1, 3, or 7 days, changing the buffer twice every day. After the wash periods, the ACSs were incubated with the streptavidin-peroxidase polymer. $n = 3$ for each condition.

Alkaline phosphatase activity and proliferation assays on cell cultures

To determine the effect of the CBD-RGD peptide in a soluble form on cells from the osteoblastic lineage, both

MC3T3-E1 mouse preosteoblasts and rat MSCs were cultured with alpha-MEM supplemented with 10% FBS and 2 mM L-glutamine, at 37°C in a humidified atmosphere with 5% CO_2 (standard conditions). Cells were seeded on 96-well plates (Nunclon; Nunc) at a density of 7.5×10^3 cells/well and incubated for 3 h under standard conditions. Once attached to the bottom of the wells, the cells were washed with alpha-MEM with 2% FBS and 2 mM L-glutamine and incubated for an additional hour. Finally, the medium was removed from the wells and replaced by alpha-MEM with 2% FBS, 2 mM L-glutamine, 0.2 mM L-ascorbate, and CBD-RGD (0, 0.25, 1, or 4 μM). The alkaline phosphatase (ALP) activity in the cultures was determined after 4 and 10 days by washing the cells with PBS and measuring the enzymatic activity using a pNPP-based method (Sigma Fast™ p-nitrophenyl phosphate tablets; Sigma-Aldrich). Another set of cells, cultured under the same conditions, was used for determining proliferation using a tetrazolium-based kit (Cell Proliferation Kit II, XTT; Roche, Basel, Switzerland) according to the manufacturer's specifications. $n = 8$ for each condition.

Mineralization assays on cell cultures

To determine if the CBD-RGD peptide was able to promote matrix mineralization in cell cultures, both MC3T3-E1 mouse preosteoblasts and rat MSCs were seeded at a density of 2×10^5 cells/well on 12-well culture plates (Nunclon; Nunc) in alpha-MEM with 2% FBS, 2 mM L-glutamine, 0.2 mM L-ascorbate, and CBD-RGD (0, 0.25, 1, or 4 μM) and cultured for 21 days with complete medium renewals at days 7 and 14. At day 21, the mineralized nodules were stained with Alizarin red S (Sigma-Aldrich) for visualization and, finally, the dye was extracted for its spectrophotometric quantification as described by Gregory *et al.*[32] Briefly, the cells were fixed with buffered formaldehyde, stained with a 40-mM Alizarin red S solution, and extensively washed to remove the excess of stain. Afterward, the stain was extracted with acetic acid, neutralized with ammonium hydroxide, and quantified by measuring the absorbance at 405 nm. $n = 6$ for each condition.

Caspase activity in cell cultures

To determine if the soluble CBD-RGD peptide can induce apoptosis on the cells used in this work, both MC3T3-E1 mouse preosteoblasts and rat MSCs were seeded at a density of 2×10^5 cells/well on black 96-well culture plates (Nunclon; Nunc) and incubated for 3 h under standard conditions. The medium was then changed to alpha-MEM with 2% FBS, 2 mM L-glutamine, and CBD-RGD (0, 0.25, 1 or 4 μM) and the cells were incubated for another 3 h. Finally, the caspase activity in the cultures was measured using a fluorimetric Homogeneous Caspase Assay (Roche), following the manufacturer's instructions. $\lambda_{ex} = 499$, $\lambda_{em} = 521$ nm. $n = 3$ for each condition.

ICQ-IF detection of vinculin

To detect the formation of focal adhesions, both MC3T3-E1 cells and rat MSCs were seeded on 13 mm diameter coverslips (Nunc) placed in 24-well culture plates (Nunclon; Nunc) at a density of 2.5×10^4 cells/well and incubated for 3 h under standard conditions. Afterward, the medium was changed to alpha-MEM with 2% FBS and 2 mM L-glutamine for 1 h. Finally, the medium was changed to alpha-MEM with 2% FBS, 2 mM L-glutamine, and CBD-RGD (0 or 4 μM) and the cells were incubated for 1 or 4 days to allow them to establish focal adhesions. HeLa cells were cultured in the DMEM (Sigma-Aldrich) with 10% FBS and 2 mM L-glutamine and seeded at the same density to be used as both positive and negative controls.

For immunostaining, the cells were fixed with 4% paraformaldehyde and permeabilized with 0.5% Triton X-100. Vinculin, one of the constituents of focal adhesion, was detected using a monoclonal mouse IgG antibody at 0.2 μg/mL and a goat anti-mouse IgG conjugated to Alexa 488. Phalloidin conjugated to TRITC was used for staining the actin filaments within the cells and their nuclei were stained with Hoechst. HeLa negative control cells were incubated without the anti-vinculin antibody or phalloidin-TRITC. Finally, the cells were viewed under a confocal microscope with a 63× objective.

Animal surgery

General animal care and surgical procedures were according to the national (RD 1201/2005) and international laws (Directive 2010/63/EU) concerning the protection of animals used for scientific purposes and were previously approved by the Ethics Committee of the University of Malaga. Twelve young (3 months old) male Wistar rats were used for this study and both animal housing and surgery were performed at the animal house facilities of the University of Malaga. An absorbable collagen sponge sheet was cut into disks (5 mm diameter, 1 mm thickness), loaded with 300 ng BMP-2, 5 μg CBD-RGD, or 300 ng BMP-2 + 5 μg CBD-RGD and let to dry for 1 h in a laminar flow cabinet before implantation. Disks incubated with vehicle only served as a negative control. Animals were anesthetized, their dorsal region was shaved and disinfected, and incisions were made in the skin to implant the ACSs into muscular pockets made in the dorsal muscles. After surgery, animals were housed in individual cages with unlimited access to food and water. Half of the animals were sacrificed 14 days after surgery, whereas the rest were sacrificed at day 21. At each time point, the ectopic implants were dissected from the surrounding tissues and used for calcium measurement ($n = 6$ for each condition) or histological analysis ($n = 3$ for each condition).

Histological analysis of the *in vivo* samples

The ectopic implants extracted for histological analysis were fixed in a 4% neutral buffered formaldehyde solution for 18 h, decalcified with Decalcifier II (Surgipath, Richmond, IL) for 4 h, and embedded in paraffin. Ten micrometer thick transversal sections were made and stained with hematoxylin–eosin (H–E) or used for immunohistochemistry using an anti-osteopontin antibody and a biotinylated anti-mouse IgG antibody. Antibody detection was performed using the ABC method (ABC Staining Kit; Pierce) and diaminobenzidine (Sigma-Aldrich) as an electron donor.

Calcium measurement in ectopic bone

The ectopic samples extracted for the measurement of their calcium content were washed with 0.9% NaCl for 2 h with several changes to remove the excess of blood. Each

implant was then incubated for 24 h at room temperature in 0.5 mL of 10% HCl to solubilize all the calcium present in the implants. Ten microliters of each sample were taken to measure its calcium content using an *o*-cresolphthalein complexone-based colorimetric method (Calcium-oC v/v, Labkit; Chemelex, Barcelona, Spain).

Statistical analysis

All data are represented as the mean values ± standard deviations. Statistical analyses of the data obtained for the *in vitro* assays were performed using the Student's *t*-test, comparing each condition with the control (zero growth factors) condition at the same time point. Analysis of the data obtained for the measurement of calcium in the ectopic bone samples was performed using the Student's *t*-test, comparing the two conditions at each time point. All analyses were made using SigmaPlot 11.0.

Results

Saturation of ACSs with CBD-RGD

Washing of the ACSs that had been loaded with 1 μg of CBD-RGD resulted in loss of the unbound molecules with

the first 30 μL of buffer volume (Fig. 1A, B). The total amount of peptide that was lost after washing was 0.224 μg and, thus, an average of 0.776 μg (458 pmol) remained in each ACS. Referred to the volume of the sponges, this amount is equivalent to an ∼23-μM concentration of the peptide.

However, washing of the ACSs that had been loaded with 5 μg of CBD-RGD resulted in a sequential loss of the unbound molecules with the first 75 μL of buffer volume (Fig. 1C, D). In this case, the total amount of peptide that was lost after washing was 4.044 μg, indicating that a 5-mm diameter ACS can retain approximately up to 0.956 μg (564 pmol) of CBD-RGD. Referred to the volume of the sponges, this amount is equivalent to an ∼29-μM concentration of the peptide.

When washing the ACSs for long periods (1, 3, or 7 days), no remarkable loss of peptides could be detected (Fig. 1E), indicating that the binding of the CBD-RGD peptide to the sponges is stable over time.

Alkaline phosphatase activity and proliferation assays on cell cultures

On MC3T3-E1 mouse preosteoblasts, the presence of CBD-RGD in a soluble form in the culture medium resulted in a
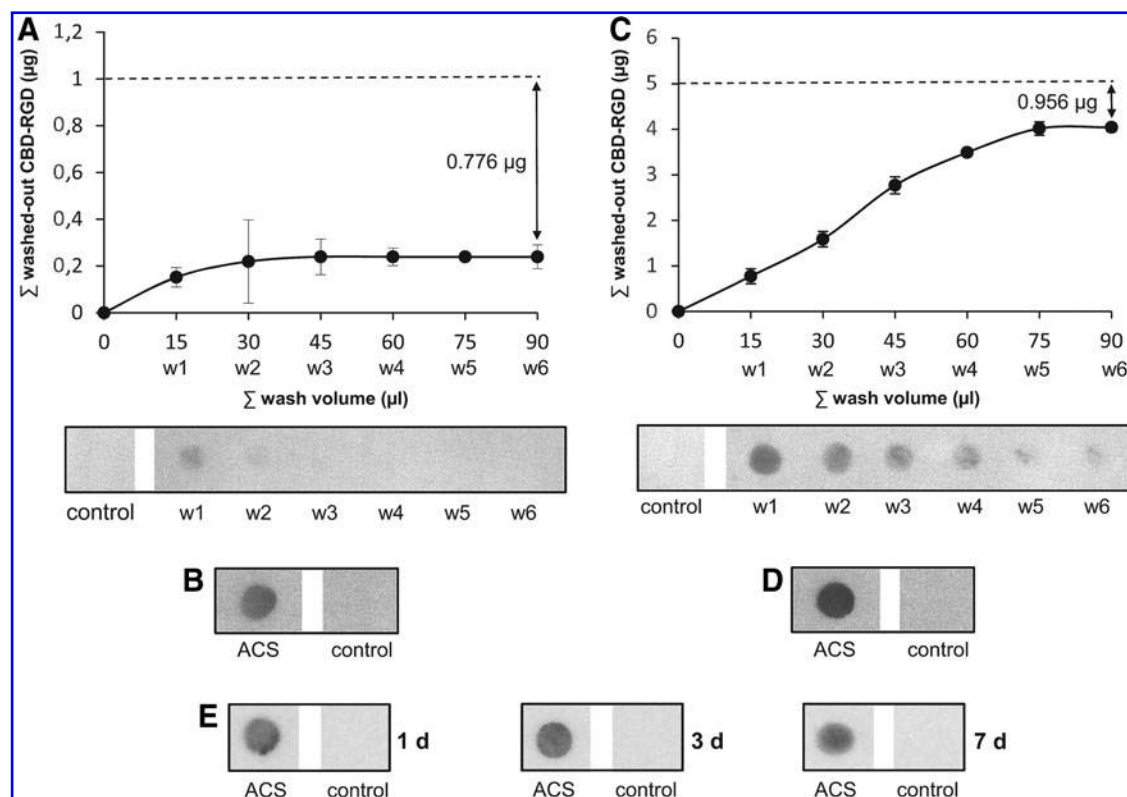

FIG. 1. Binding of the collagen-targeted RGD biomimetic (CBD-RGD) peptide to absorbable collagen type I sponges (ACSs). **(A, C)** One or 5 μg of CBD-RGD, respectively, were loaded on ACSs, which were afterward washed six times with 15 μL of phosphate-buffered saline (PBS). The washed-out peptide in each wash fraction was spectrophotometrically quantified at 205 nm. The graphics represent the total amount of peptide (mean ± SD) recovered from the sponges after each wash. $n = 4$ for each condition. **(B, D)** One or 5 μg of biotinylated CBD-RGD, respectively, were loaded on ACSs, which were afterward washed six times with 15 μL of PBS. The peptides in each wash fraction, as well as the peptides that remained bound to the ACSs, were detected using a streptavidin-peroxidase polymer. **(E)** One microgram of biotinylated CBD-RGD was loaded on ACSs, which were washed extensively with PBS for 1, 3, or 7 days. The peptides that remained bound to the ACSs were detected using a streptavidin-peroxidase polymer. $n = 3$ for each condition. RGD, arginine-glycine-aspartic acid.

dose-dependent induction of the ALP activity at both day 4 and 10 (Fig. 2A). Only at day 10, the lowest concentration of peptide tested (0.25 μM) caused a slight inhibition of ALP when compared to the control cultures. Similarly, on rat MSCs, soluble CBD-RGD was able to augment the ALP activity in the cultures at day 4 in a dose-dependent manner, while only the highest concentration (4 μM) induced a significant increment at day 10 and the lower concentrations caused a slight inhibition (Fig. 2B). Nevertheless, the effect of CBD-RGD was much less drastic on these cells due to their strong natural tendency toward differentiation when cultured *in vitro*.

The CBD-RGD peptide did not affect the growth of MC3T3-E1 cells (Fig. 2C). In contrast, when MSCs were cultured in the presence of the soluble peptide, a not significant, but remarkable lowering of cell numbers could be observed at day 4, compared with the control cultures (Fig. 2D). However, this tendency clearly switched at longer times since, at day 10, the cultures with 4 μM CBD-RGD contained a higher cell number than the controls.

Mineralization assays on cell cultures

Culturing MC3T3-E1 cells with CBD-RGD in the soluble form did not favor matrix mineralization after 21 days. In fact, although no visible signs of mineralization could be found in the control wells without peptide and the amount of dye that could be measured after its resolubilization was very low, the levels measured corresponding to cells that had been cultured with CBD-RGD were even lower, especially

with 1 μM of peptide (Fig. 3A, C). In contrast, rat MSCs have a much higher tendency toward matrix mineralization, and some disperse calcified nodules stained with Alizarin red could be seen in some of the control wells after 21 days. When the rat MSCs were cultured with CBD-RGD, both proliferation and matrix mineralization seemed to be enhanced, since these cells had formed a multilayer ring in most of the wells, with large areas of mineralization (Fig. 3B, D). The induction of matrix mineralization by CBD-RGD showed a clear trend, increasing with the concentration of peptides in the culture medium, reaching an almost threefold increase with 4 μM of peptide when compared to the controls.

Caspase activity in cell cultures

After 3 h of incubation in the presence of soluble CBD-RGD peptides, no significant changes in the caspase activity could be detected in the rat MSC cultures compared with the cells cultured without peptides (Fig. 4B). Surprisingly, the MC3T3-E1 mouse preosteoblasts showed slightly, but significantly lower levels of caspase activity when incubated with 1 or 4 μM CBD-RGD for 3 h, compared with the control cultures (Fig. 4A).

ICQ-IF detection of vinculin

After 1 day of incubation, both MC3T3-E1 cells (Fig. 5A, B) and rat MSCs (Fig. 5E, F) showed high levels of soluble vinculin in their cytoplasm and the typical accumulations of vinculin associated to bundles of actin filaments at the edges
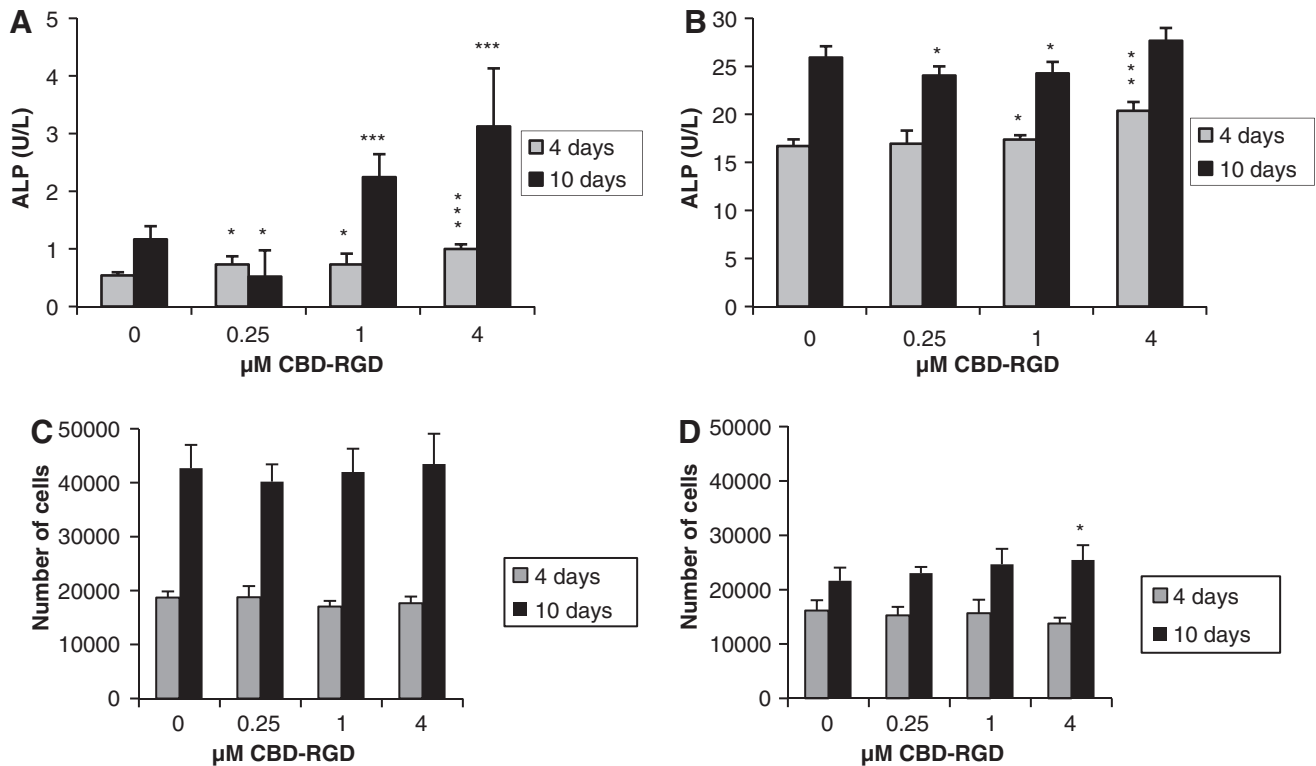

FIG. 2. Alkaline phosphatase (ALP) activity and cell growth of MC3T3-E1 (**A, C,** respectively) or rat mesenchymal stem cells (MSCs) (**B, D,** respectively) in response to CBD-RGD in soluble form. $n = 8$; *$p \leq 0.05$; ***$p \leq 0.001$. All comparisons are against the control condition for the same time point.
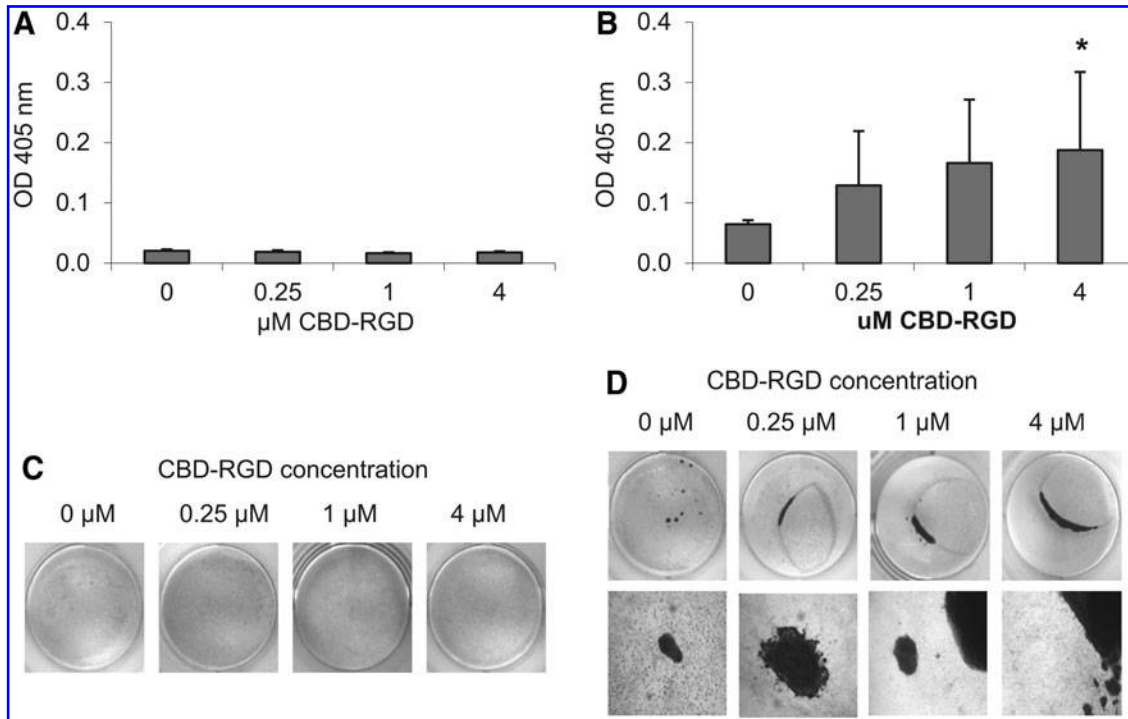
FIG. 3. Matrix mineralization by MC3T3-E1 **(A, C)** or rat MSCs **(B, D)** in response to CBD-RGD in soluble form. $n=6$; $*p \leq 0.05$.

of the cells, corresponding to focal adhesions. Whereas no differences in the number of focal adhesions could be observed in the rat MSCs cultured with or without CBD-RGD (Fig. 5E–H), MC3T3-E1 cells seemed to have responded to the CBD-RGD peptide, increasing their number of focal adhesions (Fig. 5A–D), although no quantification was made.

In vivo ectopic bone formation

The control ACSs, loaded with vehicle only, could not be recovered at any time point due to complete resorption of the sponges. Those that had been loaded with only CBD-RGD gave rise to a dense, fibrous tissue with no signs of osteogenesis (data not shown), indicating that the peptide alone was not able to induce the bone formation process in a muscular environment. The sponges loaded with 300 ng of BMP-2 did also not show clear signs of osteogenesis 14 or 21 days after surgery (Fig. 6A, B). Although the appearance of

the tissue at day 14 somehow resembled the early stages of ectopic osteogenesis, with great infiltration by cells and the formation of strongly eosinophillic extracellular material, the implants were not able to progress toward bone formation, and no clear trabecular organization could be observed at day 21. In these implants, the expression of osteopontin was not focalized in specific areas, but was rather limited to small groups of cells randomly dispersed throughout the sponges (Fig. 6C, D). In contrast, the ACSs that had been loaded with BMP-2+CBD-RGD did already show bone trabeculae at day 14, with clearly defined osteocytes within the mineralized matrix (Fig. 6E). Although these implants did not make great progression after another week, trabeculae with a mature appearance could still be found throughout them (Fig. 6F). This observation correlated well with the expression of osteopontin, which was highest at day 14 but decreased at day 21 (Fig. 6G, H). Nevertheless, this marker could still be found extensively expressed nearby the remaining trabeculae,
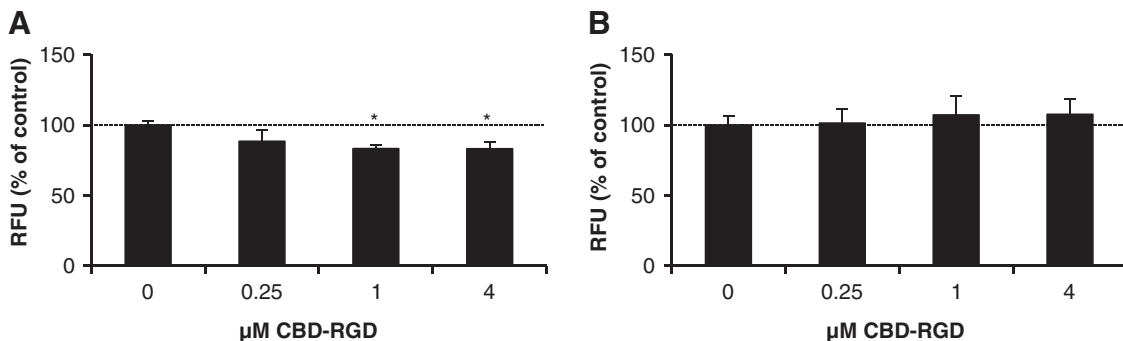

FIG. 4. Caspase activity in MC3T3-E1 **(A)** and rat MSC **(B)** cultures in response to CBD-RGD in soluble form. $n=3$; $*p \leq 0.05$. RFU, relative fluorescence unit.
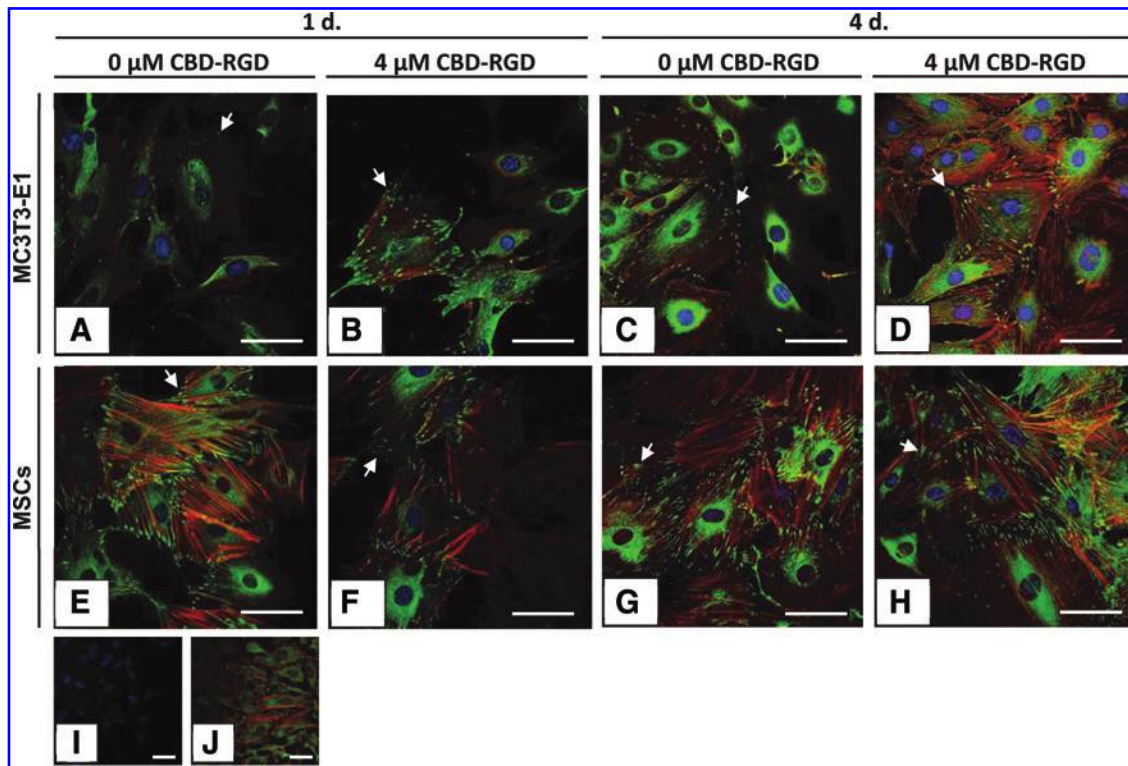
FIG. 5. Anti-vinculin fluorescence immunocytochemistry on MC3T3-E1 **(A–D)** and rat MSCs **(E–H)** cultured with or without 4 μM soluble CBD-RGD for 1 or 4 days. HeLa cells were used as negative and positive control **(I, J,** respectively). Green, vinculin; Red, F-actin; Blue, nuclei. Arrows, focal adhesions. Scale bars: 50 μm. Color images available online at www.liebertpub.com/tea

indicating that an active process of osteogenesis was still taking place at these areas.

When analyzing the calcium content of these implants, no deposited calcium could be detected for the ACSs loaded with only BMP-2 at any time point. In contrast, the implants loaded with BMP-2 + CBD-RGD did already have detectable amounts of calcium at day 14, and this amount experienced an eightfold increase after another week (Fig. 7).

Discussion

BMPs are strong osteoinductive proteins, and have pleiotropic biological effects on many other tissues than bone. On the other side, collagen is the most abundant protein in the animal ECM and is the only carrier approved to be used, in combination with BMP-2 or- 7, for clinical bone repair purposes. Due to its low natural affinity to collagen, BMP-2 must be used at much higher concentrations (1.5 mg/mL ACS) than its physiological levels, what may cause adverse side effects, such as osteoclastic resorption[33] or nonhomogenous ossification, resulting in a loss of mechanical strength.[34] In addition, the presence of anti-BMP-2 antibodies in some patients treated with this growth factor has been reported.[3] With the aim of reducing the amount of BMP-2 needed to promote osteogenesis *in vivo*, we previously designed a collagen-targeted BMP-2 to allow the functionalization of the ACSs frequently used as BMP-2-delivering and osteoconductive biomaterial. This so-called rhBMP2-CBD was able to induce bone formation at lower doses than the native BMP-2.[10] Nevertheless, producing a modified rhBMP-2 molecule with a biological activity in *Escherichia coli* is not a

cheap or simple task, and implies numerous folding and purification steps with a high percentage of protein loss during the process. Trying to overcome these inconveniences, we have now designed a synthetic CBD-RGD peptide, which is easy and cheap to obtain in large quantities. The collagen-binding properties of this peptide help to overcome the problems associated with the chemical linking of functional RGD peptides to the collagen scaffold, which implies numerous manipulations of the ACSs before their implantation, making these approaches unsuitable for clinical orthopedics. Furthermore, the CBD of the peptide not only allows its binding to the collagen fibers, but might also act as a support for the RGD domain, helping in its presentation to the cell integrins and allowing its flexible movement in the biological environment.[35] At last, it could be speculated that the CBD might also help to avoid the dispersion of unbound or released CBD-RGD peptides after implantation of the functionalized sponges, since these molecules may find a second change for attaching when they face the patient's own collagen type I fibers of the target tissue. It should be noticed that, although the α_1 and α_2 polypeptides that form collagen type I contain RGD motifs, these are inaccessible for integrins when collagen is in its native conformation.[36]

The fact that the CBD sequence might act as a support for the RGD domain could be the explanation for the effects on MSCs observed after incubation with the CBD-RGD peptide in soluble form, which induced a significant enhancement of matrix mineralization by these cells. During the first days of incubation, when the cells have still not synthesized an ECM, the soluble CBD-RGD peptide might be able to trigger
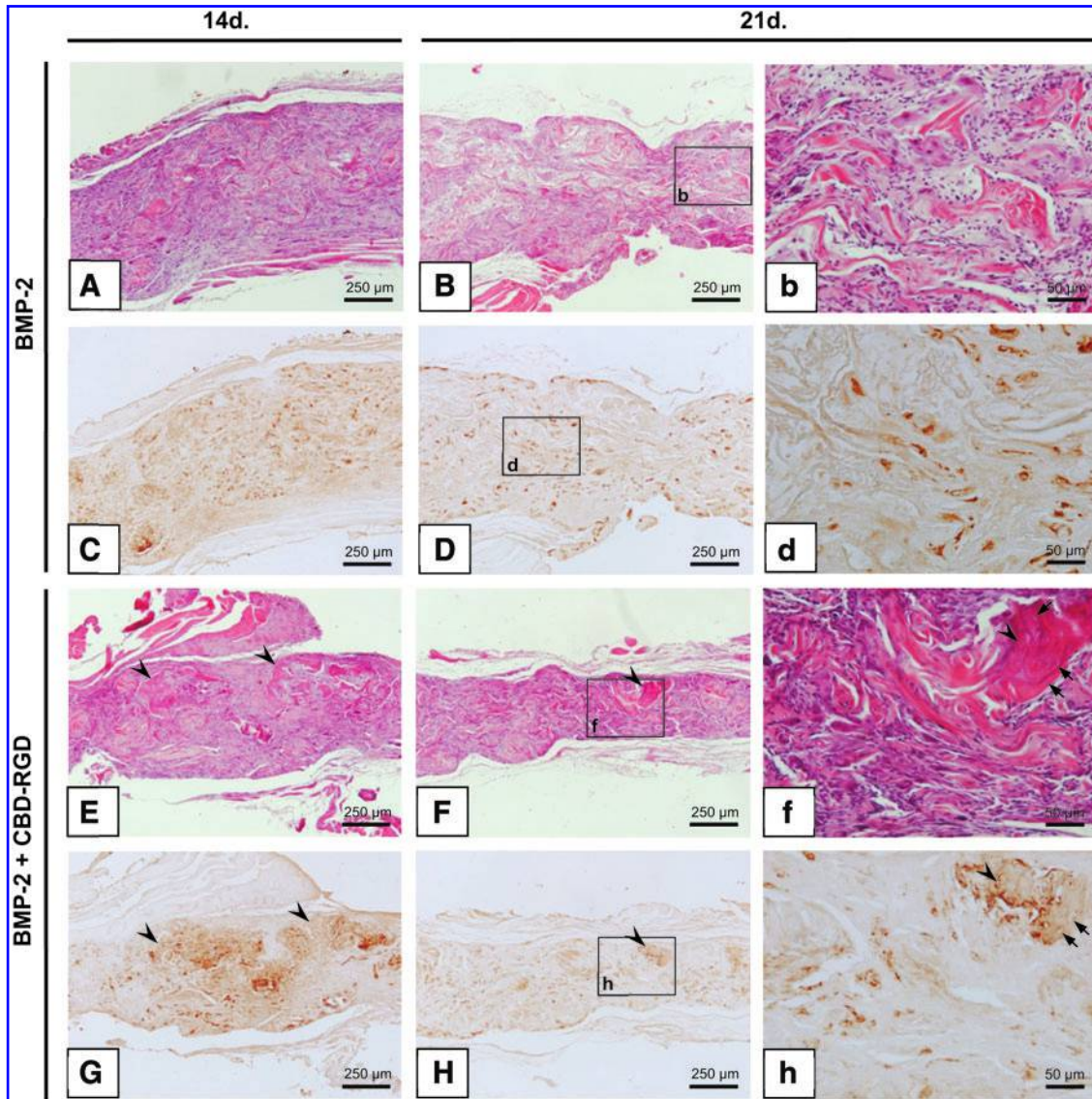
FIG. 6. Ectopic bone formation *in vivo*. Ten micrometer slices stained with H-E **(A, B, E,** and **F)** or used for detection of osteopontin by immunohistochemistry **(C, D, G,** and **H). (A–D)** ACSs loaded with 300 ng bone morphogenetic protein (BMP)-2, recovered 14 and 21 days after surgery, respectively. **(E–H)** ACSs loaded with 300 ng BMP-2 +5 μg CBD-RGD, recovered 14 and 21 days after surgery, respectively. Images **(b, d, f,** and **h)** are details of **(B, D, F,** and **H)**, respectively. Arrows, osteocytes; arrowheads, bone trabeculae. Color images available online at www.liebertpub.com/tea

integrin-dependent signaling pathways to direct cell differentiation, as it has been shown that soluble RGD peptides can bind to integrins.[37] Later on, once a collagenic matrix has been secreted by these cells, the biomimetic peptide might bind to these collagen molecules to also favor cell-ECM interactions through focal adhesion formation and continuing to direct cell differentiation. This latter hypothesis could explain the reduced ALP activity seen when MC3T3-E1 or rat MSCs were cultured with low (0.25 or 1 μM) concentrations of CBD-RGD for 10 days. It is not likely that the cells can produce sufficient ECM in such period to allow all the CBD-RGD molecules to attach to collagen fibers, and the free peptides might be blocking the cell integrins, preventing them from establishing interactions with the forming ECM. In this case, higher pressures of CBD-RGD were needed to trigger a cellular response in terms of differentiation, as seen

when using a 4-μM concentration. This is also consistent with the results obtained from the proliferation assay with MSCs: at day 4, soluble CBD-RGD binding to the cell's integrins might be preventing them from establishing interactions with the culture plastic and from proliferating to a certain extent; in contrast, at day 10, when there is sufficient collagen secreted by the cells present in the cultures, the CBD-RGD might be now attaching to this ECM, favoring cell-ECM interactions and proliferation. This effect is more drastic with MSCs than with MC3T3-E1 preosteoblasts, since the former are much more active in secreting ECM *in vitro*.

Although several studies have reported that soluble RGD peptides can induce apoptosis of different cell types through direct activation of caspase-3,[38] we have not found this effect on the cells used in this work at the concentrations of CBD-RGD used *in vitro*.
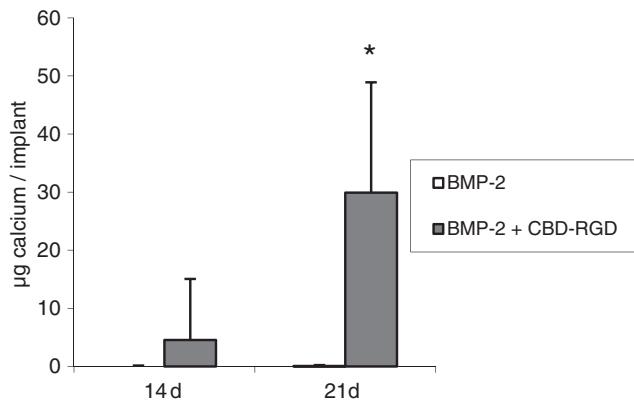
FIG. 7. Calcium content of ectopic bone formed in ACSs loaded with 300 ng BMP-2 or 300 ng BMP-2 + 5 μg CBD-RGD, 14 and 21 days after implantation. $n=6$; $*p \leq 0.01$. Note that the value of the bars that correspond to BMP-2 is zero at both time points.

It should be noticed that the cells used in the *in vitro* experiments were cultured with 2% FBS. Although fibronectin is relatively abundant in serum ($\sim 300\,\mu g/mL$) and each molecule contains one RGD sequence, the final concentration of fibronectin in the used media was $\sim 0.013\,\mu M$. Hence, the concentrations of CBD-RGD tested were between 19 and 307 times higher than the concentration of fibronectin. Keeping its percentage as low as possible, serum was added to the culture media to better mimic the cell's *in vivo* microenvironment and provide them nutrients and growth factors necessary for their differentiation. Since fibronectin was also present in the control cultures, the differences between these and the experimental cultures can only be attributed to the CBD-RGD peptide.

When ACSs loaded with BMP-2 are implanted ectopically to induce bone formation, the minimum dose necessary to observe some response has been shown to be 460 ng.[15] In fact, when 300 ng of BMP-2 were used, no histological signs of bone formation could be detected at day 21 postsurgery nor could calcium be measured in these implants, as had been described previously in the same system.[39] In contrast, when this subfunctional dose of BMP-2 was combined with the CBD-RGD peptide, the implants were able to develop bone trabeculae and to accumulate calcium deposits. Hence, it is clear that the addition of the CBD-RGD peptide has a positive effect on the osteogenic process. Since, at their respective studied doses, neither BMP-2 nor CBD-RGD alone were able to induce ectopic bone formation, it is suitable to speak about a real synergism between these two stimuli. Nevertheless, whether the CBD-RGD peptide promotes osteogenesis in this system by recruiting and attaching the host's cells to the collagen scaffold, by triggering their osteoblastic differentiation through integrin-dependent signaling pathways, or by both mechanisms is still to be determined in future studies.

Conclusion

In conclusion, the present study describes for the first time the design and characterization of a CBD-RGD peptide for the easy functionalization of ACSs. This CBD-RGD peptide is able to enhance the expression of the osteogenic marker ALP and matrix mineralization by MSCs and, when combined with a subfunctional dose of BMP-2 on ACSs, to augment *in vivo* ectopic osteogenesis and calcification levels of the implants. These properties suggest that this peptide might be a helpful tool to reduce the doses of BMPs currently used in orthopedic surgery.

Disclosure Statements

No competing financial interests exist.

References

1. Friedlaender, G.E., Perry, C.R., Cole, J.D., Cook, S.D., Cierny, G., Muschler, G.F., Zych, G.A., Calhoun, J.H., LaForte, A.J., and Yin, S. Osteogenic protein-1 (bone morphogenetic protein-7) in the treatment of tibial nonunions. J Bone Joint Surg Am **83-A Suppl 1,** S151, 2001.
2. Boden, S.D., Kang, J., Sandhu, H., and Heller, J.G. Use of recombinant human bone morphogenetic protein-2 to achieve posterolateral lumbar spine fusion in humans: a prospective, randomized clinical pilot trial: 2002 Volvo Award in clinical studies. Spine **27,** 2662, 2002.
3. Govender, S., Csimma, C., Genant, H.K., Valentin-Opran, A., Amit, Y., Arbel, R., Aro, H., Atar, D., Bishay, M., Börner, M.G., Chiron, P., Choong, P., Cinats, J., Courtenay, B., Feibel, R., Geulette, B., Gravel, C., Haas, N., Raschke, M., Hammacher, E., van der Velde, D., Hardy, P., Holt, M., Josten, C., Ketterl, R.L., Lindeque, B., Lob, G., Mathevon, H., McCoy, G., Marsh, D., Miller, R., Munting, E., Oevre, S., Nordsletten, L., Patel, A., Pohl, A., Rennie, W., Reynders, P., Rommens, P.M., Rondia, J., Rossouw, W.C., Daneel, P.J., Ruff, S., Rüter, A., Santavirta, S., Schildhauer, T.A., Gekle, C., Schnettler, R., Segal, D., Seiler, H., Snowdowne, R.B., Stapert, J., Taglang, G., Verdonk, R., Vogels, L., Weckbach, A., Wentzensen, A., Wisniewski, T., and BMP-2 Evaluation in Surgery for Tibial Trauma (BESTT) Study Group. Recombinant human bone morphogenetic protein-2 for treatment of open tibial fractures: a prospective, controlled, randomized study of four hundred and fifty patients. J Bone Joint Surg Am **84-A,** 2123, 2002.
4. Vaccaro, A.R., Patel, T., Fischgrund, J., Anderson, D.G., Truumees, E., Herkowitz, H.N., Phillips, F., Hilibrand, A., Albert, T.J., Wetzel, T., and McCulloch, J.A. A pilot study evaluating the safety and efficacy of OP-1 Putty (rhBMP-7) as a replacement for iliac crest autograft in posterolateral lumbar arthrodesis for degenerative spondylolisthesis. Spine **29,** 1885, 2004.

5. Swiontkowski, M.F., Aro, H.T., Donell, S., Esterhai, J.L., Goulet, J., Jones, A., Kregor, P.J., Nordsletten, L., Paiement, G., and Patel, A. Recombinant human bone morphogenetic protein-2 in open tibial fractures. A subgroup analysis of data combined from two prospective randomized studies. J Bone Joint Surg Am **88,** 1258, 2006.

6. Garrison, K.R., Donell, S., Ryder, J., Shemilt, I., Mugford, M., Harvey, I., and Song, F. Clinical effectiveness and cost-effectiveness of bone morphogenetic proteins in the non-healing of fractures and spinal fusion: a systematic review. Health Technol Assess **11,** 1, 2007.

7. Granjeiro, J.M., Oliveira, R.C., Bustos-Valenzuela, J.C., Sogayar, M.C., and Taga, R. Bone morphogenetic proteins: from structure to clinical use. Braz J Med Biol Res **38,** 1463, 2005.

8. Seeherman, H.J., Bouxsein, M., Kim, H., Li, R., Li, X.J., Aiolova, M., and Wozney, J.M. Recombinant human bone morphogenetic protein-2 delivered in an injectable calcium phosphate paste accelerates osteotomy-site healing in a nonhuman primate model. J Bone Joint Surg Am **86-A,** 1961, 2004.

9. Hulsart-Billström, G., Hu, Q., Bergman, K., Jonsson, K.B., Berg, J., Tang, R., Larsson, S., and Hilborn, J. Calcium phosphates compounds in conjunction with hydrogel as carrier for BMP-2: a study on ectopic bone formation in rats. Acta Biomater **7,** 3042, 2011.

10. Visser, R., Arrabal, P.M., Becerra, J., Rinas, U., and Cifuentes, M. The effect of an rhBMP-2 absorbable collagen sponge-targeted system on bone formation *in vivo*. Biomaterials **30,** 2032, 2009.

11. Akita, S., Fukui, M., Nakagawa, H., Fujii, T., and Akino, K. Cranial bone defect healing is accelerated by mesenchymal stem cells induced by coadministration of bone morphogenetic protein-2 and basic fibroblast growth factor. Wound Repair Regen **12,** 252, 2004.

12. Kakudo, N., Kusumoto, K., Kuro, A., and Ogawa, Y. Effect of recombinant human fibroblast growth factor-2 on intramuscular ectopic osteoinduction by recombinant human bone morphogenetic protein-2 in rats. Wound Repair Regen **14,** 336, 2006

13. Kempen, D.H., Lu, L., Heijink, A., Hefferan, T.E., Creemers, L.B., Maran, A., Yaszemski, M.J., and Dhert, W.J. Effect of local sequential VEGF and BMP-2 delivery on ectopic and orthotopic bone regeneration. Biomaterials **30,** 2816, 2009.

14. Huang, Z., Ren, P.G., Ma, T., Smith, R.L., and Goodman, S.B. Modulating osteogenesis of mesenchymal stem cells by modifying growth factor availability. Cytokine **51,** 305, 2010.

15. Wang, E.A., Rosen, V., D'Alessandro, J.S., Bauduy, M., Cordes, P., Harada, T., Israel, D.I., Hewick, R.M., Kerns, K.M., LaPan, P., Luxenberg, D.P., McQuaid, D., Moutsatsos, I.K., Nove, J., and Wozney, J.M. Recombinant human bone morphogenetic protein induces bone formation. Proc Natl Acad Sci USA **87,** 2220, 1990.

16. Volek-Smith, H., and Urist, M.R. Recombinant human bone morphogenetic protein (rhBMP) induced heterotopic bone development *in vivo* and *in vitro*. Proc Soc Exp Biol Med **211,** 265, 1996.

17. García, A.J., and Reyes, C.D. Bio-adhesive surfaces to promote osteoblast differentiation and bone formation. J Dent Res **84,** 407, 2005.

18. Le Guillou-Buffello, D., Bareille, R., Gindre, M., Sewing, A., Laugier, P., and Amédée, J. Additive effect of RGD coating to functionalized titanium surfaces on human osteopro-

19. genitor cell adhesion and spreading. Tissue Eng Part A **14,** 1445, 2008.

19. Germanier, Y., Tosatti, S., Broggini, N., Textor, M., and Buser, D. Enhanced bone apposition around biofunctionalized sandblasted and acid-etched titanium implant surfaces. A histomorphometric study in miniature pigs. Clin Oral Implants Res **17,** 251, 2006.

20. Petrie, T.A., Raynor, J.E., Reyes, C.D., Burns, K.L., Collard, D.M., and García, A.J. The effect of integrin-specific bioactive coatings on tissue healing and implant osseointegration. Biomaterials **29,** 2849, 2008.

21. Moore, N.M., Lin, N.J., Gallant, N.D., and Becker, M.L. Synergistic enhancement of human bone marrow stromal cell proliferation and osteogenic differentiation on BMP-2-derived and RGD peptide concentration gradients. Acta Biomater **7,** 2091, 2011.

22. Park, J.S., Yang, H.N., Jeon, S.Y., Woo, D.G., Na, K., and Park, K.H. Osteogenic differentiation of human mesenchymal stem cells using RGD-modified BMP-2 coated microspheres. Biomaterials **31,** 6239, 2010.

23. Song, D.P., Chen, M.J., Liang, Y.C., Bai, Q.S., Chen, J.X., and Zheng, X.F. Adsorption of tripeptide RGD on rutile TiO(2) nanotopography surface in aqueous solution. Acta Biomater **6,** 684, 2010.

24. Ferris, D.M., Moodie, G.D., Dimond, P.M., Gioranni, C.W., Ehrlich, M.G., and Valentini, R.F. RGD-coated titanium implants stimulate increased bone formation *in vivo*. Biomaterials **20,** 2323, 1999.

25. Oya, K., Tanaka, Y., Saito, H., Kurashima, K., Nogi, K., Tsutsumi, H., Tsutsumi, Y., Doi, H., Nomura, N., and Hanawa, T. Calcification by MC3T3-E1 cells on RGD peptide immobilized on titanium through electrodeposited PEG. Biomaterials **30,** 1281, 2009.

26. Roessler, S., Born, R., Scharnweber, D., Worch, H., Sewing, A., and Dard, M. Biomimetic coatings functionalized with adhesion peptides for dental implants. J Mater Sci Mater Med **12,** 871, 2001.

27. Zhang, L., Hum, M., Wang, M., Li, Y., Chen, H., Chu, C., and Jiang, H. Evaluation of modifying collagen matrix with RGD peptide through periodate oxidation. J Biomed Mater Res A **73,** 468, 2005.

28. Monteiro, G.A., Fernandes, A.V., Sundararaghavan, H.G., and Shreiber, D.I. Positively and negatively modulating cell adhesion to type I collagen via peptide grafting. Tissue Eng Part A **17,** 1663, 2011.

29. Tuan, T.L., Cheung, D.T., Wu, L.T., Yee, A., Gabriel, S., Han, B., Morton, L., Nimni, M.E., and Hall, F.L. Engineering, expression and renaturation of targeted TGF-beta fusion proteins. Connect Tissue Res **34,** 1, 1996.

30. Han, B., Hall, F.L., and Nimni, M.E. Refolding of a recombinant collagen-targeted TGFbeta2 fusion protein expressed in *Escherichia coli*. Protein Expr Purif **11,** 169, 1997.

31. Andrades, J.A., Wu, L.T., Hall, F.L., Nimni, M.E., and Becerra, J. Engineering, expression, and renaturation of a collagen-targeted human bFGF fusion protein. Growth Factors **18,** 261, 2011.

32. Gregory, C.A., Gunn, W.G., Peister, A., and Prockop, D.J. An Alizarin red-based assay of mineralization by adherent cells in culture: comparison with cetylpyridinium chloride extraction. Anal Biochem **329,** 77, 2004.

33. Itoh, K., Udagawa, N., Katagiri, T., Iemura, S., Ueno, N., Yasuda, H., Higashio, K., Quinn, J.M., Gillespie, M.T., Martin, T.J., Suda, T., and Takahashi, N. Bone morphogenetic protein 2 stimulates osteoclast differentiation and sur-

vival supported by receptor activator of nuclear factor-kappaB ligand. Endocrinology **142,** 3656, 2001.

34. Sciadini, M.F., and Johnson, K.D. Evaluation of recombinant human bone morphogenetic protein-2 as a bone-graft substitute in a canine segmental defect model. J Orthop Res **18,** 289, 2000.

35. Shin, H., Jo, S., and Mikos, A.G. Biomimetic materials for tissue engineering. Biomaterials **24,** 4353, 2003.

36. Taubenberger, A.V., Woodruff, M.A., Bai, H., Muller, D.J., and Hutmacher, D.W. The effect of unlocking RGD-motifs in collagen I on pre-osteoblast adhesion and differentiation. Biomaterials **31,** 2827, 2010.

37. Shin, H., Jo, S., and Mikos, A.G. Modulation of marrow stromal osteoblast adhesion on biomimetic oligo[poly(ethylene glycol) fumarate] hydrogels modified with Arg-Gly-Asp peptides and a poly(ethyleneglycol) spacer. J Biomed Mater Res **61,** 169, 2002.

38. Matsuki, K., Sasho, T., Nakagawa, K., Tahara, M., Sugioka, K., Ochiai, N., Ogino, S., Wada, Y., and Moriya, H. RGD peptide-induced cell death of chondrocytes and synovial cells. J Orthop Sci **13,** 524, 2008.

39. Visser, R., Arrabal, P.M., Santos-Ruiz, L., Becerra, J., and Cifuentes, M. Basic fibroblast growth factor enhances the osteogenic differentiation induced by bone morphogenetic protein-6 *in vitro* and *in vivo*. Cytokine **58,** 27, 2012.

Address correspondence to:
Rick Visser, PhD
Andalusian Center for Nanomedicine
and Biotechnology (BIONAND)
Parque Tecnologico de Andalucia
Calle Severo Ochoa 35
Campanillas
Malaga 29590
Spain

E-mail: visser@uma.es